

Article

Structure-Dependent Spectroscopic Properties of Yb³⁺-Doped Phosphosilicate Glasses Modified by SiO₂

Ling Wang¹, Huidan Zeng^{1,*}, Bin Yang¹, Feng Ye¹, Jianding Chen¹, Guorong Chen¹, Andrew T. Smith² and Luyi Sun²

- ¹ Key Laboratory for Ultrafine Materials of Ministry of Education, School of Materials Science and Engineering, East China University of Science and Technology, Shanghai 200237, China; y30140453@mail.ecust.edu.cn (L.W.); y45150059@mail.ecust.edu.cn (B.Y.); y30140482@mail.ecust.edu.cn (F.Y.); jiandingchen@ecust.edu.cn (J.C.); grchen@ecust.edu.cn (G.C.)
- ² Department of Chemical and Biomolecular Engineering and Polymer Program, Institute of Materials Science, University of Connecticut, Storrs, CT 06269, USA; andrew.smith@uconn.edu (A.T.S.); luyi.sun@uconn.edu (L.S.)
- * Correspondence: hdzeng@ecust.edu.cn; Tel./Fax: +86-21-6425-3395

Academic Editor: Giorgio Biasiol

Received: 30 January 2017; Accepted: 23 February 2017; Published: 28 February 2017

Abstract: Yb³⁺-doped phosphate glasses containing different amounts of SiO₂ were successfully synthesized by the conventional melt-quenching method. The influence mechanism of SiO₂ on the structural and spectroscopic properties was investigated systematically using the micro-Raman technique. It was worth noting that the glass with 26.7 mol % SiO₂ possessed the longest fluorescence lifetime (1.51 ms), the highest gain coefficient (1.10 ms·pm²), the maximum Stark splitting manifold of ²F_{7/2} level (781 cm⁻¹), and the largest scalar crystal-field N_J and Yb³⁺ asymmetry degree. Micro-Raman spectra revealed that introducing SiO₂ promoted the formation of P=O linkages, but broke the P=O linkages when the SiO₂ content was greater than 26.7 mol %. Based on the previous ²⁹Si MAS NMR experimental results, these findings further demonstrated that the formation of [SiO₆] may significantly affect the formation of P=O linkages, and thus influences the spectroscopic properties of the glass. These results indicate that phosphosilicate glasses may have potential applications as a Yb³⁺-doped gain medium for solid-state lasers and optical fiber amplifiers.

Keywords: Yb³⁺-doped; phosphosilicate glasses; SiO₂

1. Introduction

Yb³⁺-doped laser materials operating at wavelengths around 1 μm have been intensively investigated for a wide variety of applications, such as high-power and short-pulse lasers, material processing, and optical telecommunications [1–4]. Yb³⁺ ions are regarded as the main dopant for the applications because of their simple energy-level scheme, which prevents excited-state absorption and multi-phonon non-radiative decay, and obviates the possibility of concentration quenching through cross-relaxation [5]. Since the first glass laser was obtained in 1961 by Snitzer [6], Yb³⁺-doped glasses have been well established as solid-state lasers and optical fiber amplifiers for optical telecommunications. Recently, for high-power glass-based laser systems, phosphate glasses have been used as a matrix for Yb³⁺ ions because of their high rare-earth solubility, high gain coefficient and superior spectroscopic properties [7–9]. However, the predominant disadvantages of phosphate glasses are their chemical durability and thermo-mechanical limitations. Therefore, optimizing the glass compositions with significantly improved thermo-mechanical properties is required.

Silicate glasses exhibit excellent chemical durability, thermo-mechanical properties and optical properties. Recent studies have shown that the mechanical properties of phosphate glasses can be efficiently improved by doping with SiO₂ [10–12]. Chen Wei et al. [11] suggested that the introduction of SiO₂ into phosphate glasses can strengthen the thermo-mechanical properties of the glass without severely degrading the spectroscopic properties. Zhang Liyan et al. [12] reported that the spectroscopic properties of 60P₂O₅-7.5Al₂O₃-15K₂O-17.5BaO glass can be improved by the addition of SiO₂. Moreover, the Stark splitting of Yb³⁺-doped phosphate glasses is enlarged through the introduction of SiO₂, which allows the glass to achieve the laser output successfully. The glass structure and the local coordination of rare-earth ions can be effectively modulated by doping SiO₂ into phosphate glasses which critically influences the spectroscopic properties of the glass. Zeng Huidan et al. [13] reported that both the luminous intensity and luminous decay time of the glass appeared to have positive correlations with the amount of bridging oxygen of the glass matrix through using X-ray photoelectron spectroscopy (XPS). Hu Lili et al. [14] reported the mechanism for the decrease in Yb³⁺ absorption and emission intensity caused by P⁵⁺ doping. They found that Yb³⁺ coordinated to the P–O site in glass with a molar ratio of P⁵⁺/Al³⁺ ≤ 1, and coordinated to the P=O site in glass with a molar ratio of P⁵⁺/Al³⁺ > 1.

In this study, Yb³⁺-doped phosphate glasses in the system BaO-P₂O₅ were modified by the addition of SiO₂. The scalar crystal-field N_J and Yb³⁺ asymmetry degrees were calculated from the Stark splitting levels, which were derived from Lorentz fitting based on the absorption and emission spectra. Furthermore, the influence mechanism of SiO₂ on the structural and spectroscopic properties was investigated systematically using the micro-Raman technique and previous ²⁹Si MAS NMR experimental results. The results may have certain implications for the realization of a new generation of high-power solid-state lasers for optical telecommunications applications.

2. Experimental

Yb³⁺-doped silicophosphate glasses with compositions (in mol %) 20BaO-(80-*x*)P₂O₅-*x*SiO₂-1Yb₂O₃ (*x* = 9, 16, 26.7, 32, and 40 mol %, respectively) were prepared by conventional melt-quenching technique. High purity BaCO₃, NH₄H₂PO₄, SiO₂ from Sinopharm Chemical Reagent Company (Ning Bo, China), and 99.99% Yb₂O₃ from Macklin were used as starting materials for preparation of the glasses. About 20 g of raw materials were thoroughly crushed in an agate mortar and the homogeneous mixture was transferred into a corundum crucible, which was preheated at 350 °C for 30 min before being fully melted at 1350–1400 °C for 45 min under continuous stirring. Molten glass was air quenched by casting it onto a preheated brass mold to form bulk glasses and annealed at 430–480 °C for 5 h to reduce the thermal stress and strains. Then the furnace was switched off and the glass was allowed to cool down to room temperature at a cooling rate of about 3 K·min⁻¹. A slab of 10 mm × 10 mm × 2 mm sample was cut from the specimens and both sides were optically polished for the spectroscopic measurements.

The UV-VIS-NIR absorption spectra of BaO-P₂O₅-SiO₂ glasses were measured using a Varian CARY 500 spectrophotometer (Varian Inc., Palo Alto, CA, USA) in the scanning range of 800–1100 nm. With 915 nm laser diode pump, the emission spectra and lifetimes were measured by a high resolution spectrofluorometer FLSP920 cooled with liquid helium (Edinburgh Instruments Ltd., Livingston, UK). A scanning step of 1 nm was used to measure both absorption and emission spectra. The structural information on glass samples was obtained by micro-Raman spectrometer (INVIA, Renishaw, Gloucestershire, UK) with an Ar⁺-ion laser (514.5 nm) as the irradiation source. Baseline correction was performed using the Wire software program from Renishaw. All the measurements were performed at room temperature.

3. Results and Discussion

The absorption and emission spectra of 20BaO-(80-*x*)P₂O₅-*x*SiO₂-1Yb₂O₃ (*x* = 9, 16, 26.7, 32, and 40 mol %, respectively) glasses are plotted in Figure 1. As shown in this figure, the absorption band

of the ${}^2F_{5/2} \rightarrow {}^2F_{7/2}$ transition was at 975 nm which corresponds to the transition between the lowest level of the ${}^2F_{5/2}$ and ${}^2F_{7/2}$ manifolds. The absorption intensity of glass samples decreased with the increasing SiO_2 content. Under excitation with 915 nm LDs (Laser Diodes), NIR emission peaks at around 975 and 1005 nm were observed. The SiO_2 addition resulted in an increase in the emission intensity at around 975 nm. One broad emission band with the peak centered at 1005 nm was obtained upon excitation by 915 nm. The emission intensity decreased with the increased concentration of SiO_2 up to 26.7 mol %, and then increased as shown in Figure 1b. The variation trend of the luminescent intensity was different from the trend of the absorption intensity, which means other factors must exist that are able to affect the luminescent intensity.

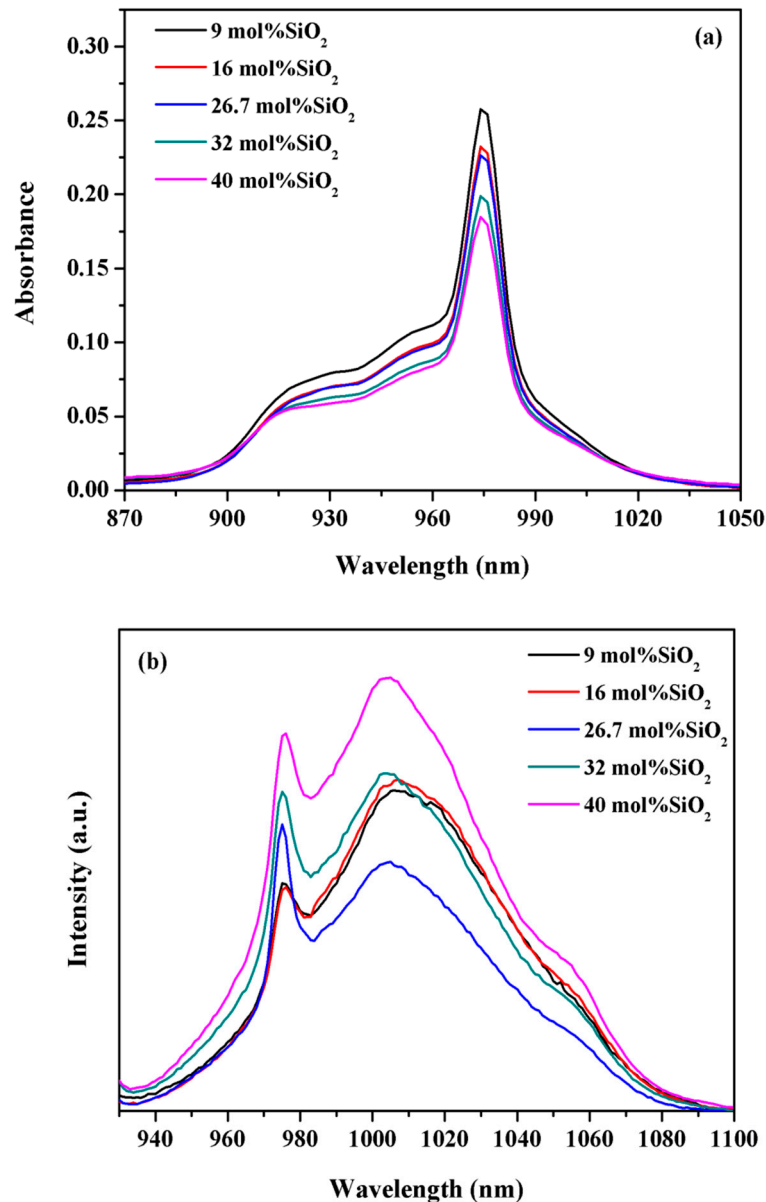


Figure 1. Absorption (a) and emission (b) spectra of $20\text{BaO}-(80-x)\text{P}_2\text{O}_5-x\text{SiO}_2-1\text{Yb}_2\text{O}_3$ ($x = 9, 16, 26.7, 32,$ and 40 mol %, respectively) glasses.

The lifetime of luminescent ions is a critical parameter for broadband optical amplifiers. The compositional dependences of emission lifetimes are shown in Figure 2. Apparently, the lifetime increases monotonically with the increase of the SiO_2 content up to 26.7 mol %, and then decreases

slightly with further increasing the content of SiO₂. Besides the lifetime, the absorption and stimulated emission cross-sections are also an important factor for solid-state lasers and broadband optical amplifiers. The absorption and emission cross-sections have been calculated by the reciprocity method [15,16]; the absolute value of cross-sections and accurate spectra information can be obtained in Table 1. As shown in Table 1, the absorption and emission cross-sections of 20BaO-(80-x)P₂O₅-xSiO₂-1Yb₂O₃ (x = 9, 16, 26.7, 32, and 40 mol %, respectively) glass samples decreased with the increasing SiO₂ concentration. The magnitude of the absorption (emission) cross-section at 975 nm for all the studied Yb³⁺-doped glass was found to be in the range of 0.62–1.09 × 10⁻²⁰ (0.83–1.46 × 10⁻²⁰ cm²), which is much higher than those of the commercial Kigre QX/Yb: 0.50 × 10⁻²⁰ (1.06 × 10⁻²⁰ cm²) laser glass [17]. The product (σ_{em} × τ_{exp}) of the stimulated emission cross-section and the lifetime is a significant parameter to depict laser materials for the laser threshold is inversely proportional to σ_{em} × τ_{exp}. The σ_{em} × τ_{exp} values of the Yb³⁺-doped phosphosilicate glass are shown in Table 1. All the σ_{em} × τ_{exp} values of this work were about 1 × 10⁻²³ cm²s, which indicates that these glasses could be a potential material for high-power solid-state lasers and broadband optical amplifiers.

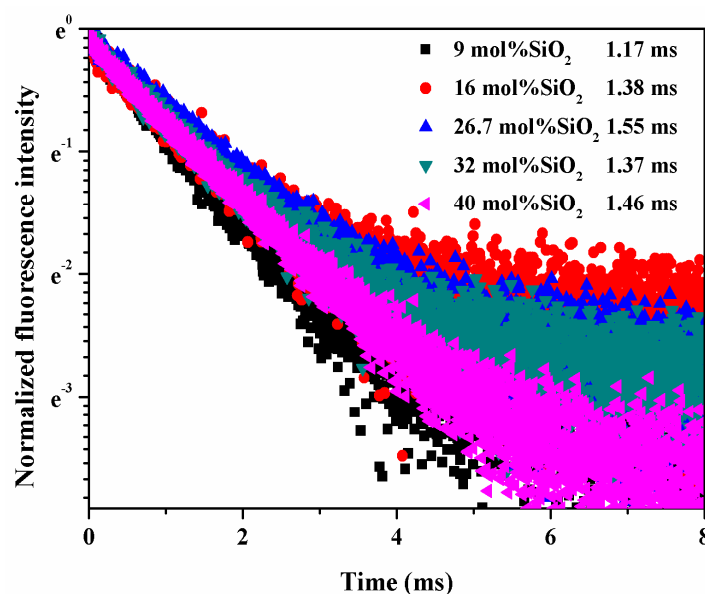


Figure 2. The fluorescence decay curve of Yb³⁺-doped 20BaO-(80-x)P₂O₅-xSiO₂-1Yb₂O₃ (x = 9, 16, 26.7, 32, and 40 mol %, respectively) glasses.

Table 1. Spectral parameters for 20BaO-(80-x)P₂O₅-xSiO₂-1Yb₂O₃ (BPSx) (x = 9, 16, 26.7, 32, and 40 mol %, respectively) glass samples.

Glass	σ _{abs} (975 nm) (10 ⁻²⁰ cm ²)	σ _{em} (975 nm) (10 ⁻²⁰ cm ²)	σ _{abs} (1005 nm) (10 ⁻²⁰ cm ²)	σ _{em} (1005 nm) (10 ⁻²⁰ cm ²)	τ _{exp} (ms)	σ _{em} × τ _{exp} (10 ⁻²⁰ cm ² ·ms)
BPS9	1.09	1.46	0.15	0.86	1.17	1.01
BPS16	0.98	1.30	0.13	0.76	1.38	1.04
BPS26.7	0.85	1.13	0.12	0.71	1.55	1.10
BPS32	0.80	1.07	0.11	0.66	1.37	0.91
BPS40	0.62	0.83	0.11	0.62	1.46	0.90

Recently, many research studies have been published on NIR luminescence in Yb³⁺-doped glasses; however, the origin of this phenomenon has not been identified. The relation between the glass structure and the spectroscopic properties of Yb³⁺-doped glass is revealed through the evaluation of

the scalar crystal-field N_J and Yb^{3+} asymmetry degree. According to References [18–20], the scalar crystal-field N_J and Yb^{3+} asymmetry degree can be calculated from the Stark splitting levels, which can be derived from Lorentz fitting based on the absorption and emission spectra. As shown in Figure 3, the maximum Stark splitting manifold of the ${}^2F_{7/2}$ level (781 cm^{-1}) and the scalar crystal-field N_J and Yb^{3+} asymmetry degree are observed when the SiO_2 concentration is 26.7 mol %.

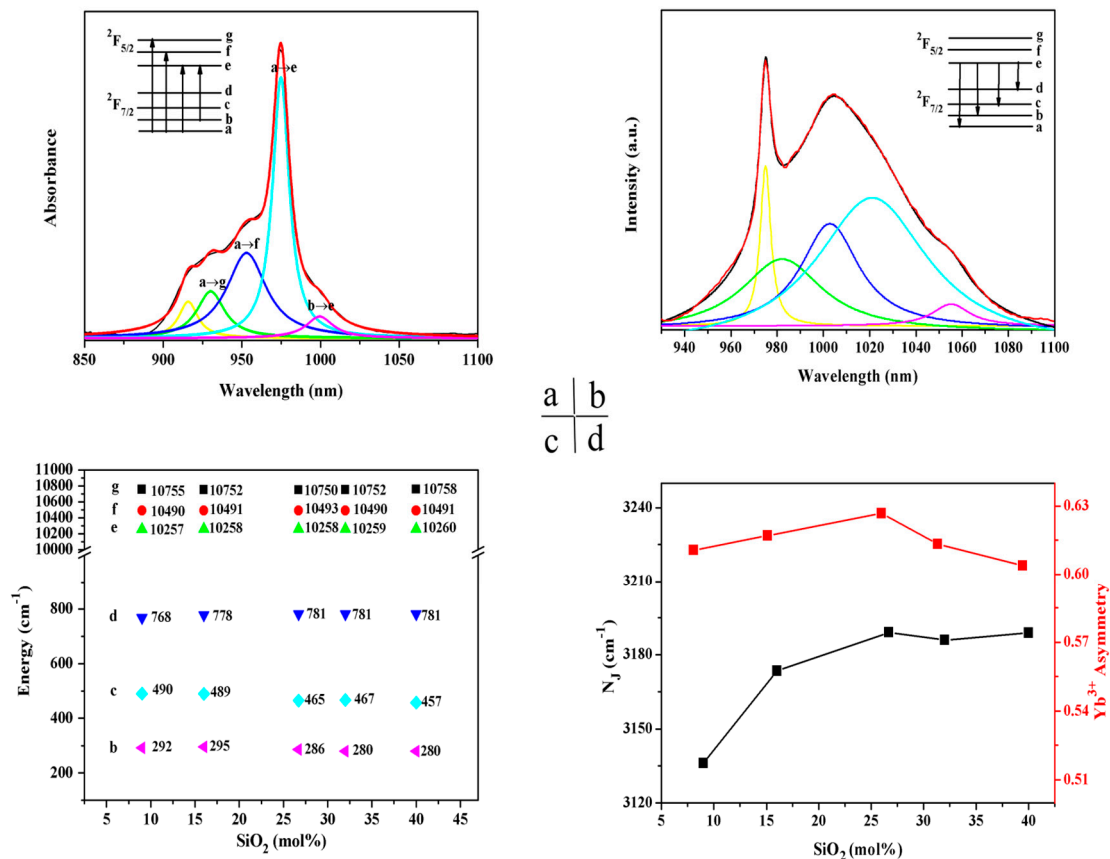


Figure 3. Lorentz peak analysis for absorption (a) and emission (b) spectra of $20\text{BaO}-53.3\text{P}_2\text{O}_5-26.7\text{SiO}_2-1\text{Yb}_2\text{O}_3$ glass (the black lines are the original spectra, while the red lines offer the fitting lines composed of the corresponding multi-fitting peaks); (c) Stark level energies of ${}^2F_{7/2}$ and ${}^2F_{5/2}$ manifolds in $20\text{BaO}-(80-x)\text{P}_2\text{O}_5-x\text{SiO}_2-1\text{Yb}_2\text{O}_3$ ($x = 9, 16, 26.7, 32,$ and 40 mol %, respectively) glasses obtained from the Lorentz fitting to the absorption and emission spectra; (d) Scalar crystal-field parameters N_J and Yb^{3+} asymmetry degree in $20\text{BaO}-(80-x)\text{P}_2\text{O}_5-x\text{SiO}_2-1\text{Yb}_2\text{O}_3$ ($x = 9, 16, 26.7, 32,$ and 40 mol %, respectively) glasses.

As is known, introducing SiO_2 into phosphate glass can effectively modulate the structure and thus lead to a change in the Yb^{3+} local field. Therefore, to further elucidate the role of SiO_2 in phosphate glass, the detailed structural information of the glass by using the micro-Raman technique was obtained. In Figure 4, micro-Raman spectra are shown as a function of an increasing SiO_2 content in the range of $200\text{--}1600\text{ cm}^{-1}$. The broad bands of the $\text{Si}^{(n)}$ units ($\text{Si}^{(n)}$ represents the $[\text{SiO}_4]$ tetrahedral unit and n is the amount of bridging oxygen per tetrahedral) with $n = 4, 3, 2, 1$ and 0 , which are centered at around $1200, 1100, 950, 900,$ and 850 cm^{-1} , respectively [21]. The spectra of low- SiO_2 glass show four major features centered near $700, 1155, 1277,$ and 1330 cm^{-1} , respectively. With an increasing content of SiO_2 , several new peaks appear at $500, 900,$ and 970 cm^{-1} . The bands near $900, 970, 1155\text{ cm}^{-1}$ are assigned to $\text{Si}^{(1)}, \text{Si}^{(2)},$ and $\text{Si}^{(4)}$, respectively. As shown in Figure 4, the band near 1155 cm^{-1} contributing to the stretching vibration mode in $\text{Si}^{(4)}$ becomes wider and moves towards a lower wave number. This may be due to the formation of $[\text{SiO}_6]$ which broadens the peak near

1155 cm^{-1} [22–24]. The band near 1330 cm^{-1} is derived from P=O stretching vibration [25,26]. As the content of SiO_2 is increased, the intensity of the Raman peak increases until 26.7 mol % SiO_2 and then it decreases. This structural change indicates that the introduction of SiO_2 can promote the formation of P=O linkages, but it can also break the P=O linkages when the SiO_2 content is greater than 26.7 mol %. P=O linkages arouse a remarkable adjustment on the distorted structure and thus result in a dramatic change in the Yb^{3+} local structure. As shown in Figure 3d, the variation trend of the asymmetry degree and N_j is similar to that of the P=O linkage. According to previous work [27], ^{29}Si MAS NMR spectra of $20\text{BaO}-(80-x)\text{P}_2\text{O}_5-x\text{SiO}_2$ ($x = 9, 16, 26.7, 32,$ and 40 mol %, respectively) glass samples indicated that $[\text{SiO}_6]$ existed in these phosphosilicate glasses, and the peaks of $[\text{SiO}_6]$ significantly decreased when the SiO_2 content was greater than 26.7 mol %. Based on the previous ^{29}Si MAS NMR and micro-Raman experimental results, these findings further demonstrate that the presence of $[\text{SiO}_6]$ may significantly affect the formation of P=O, and thus improve the spectroscopic properties of phosphate glasses.

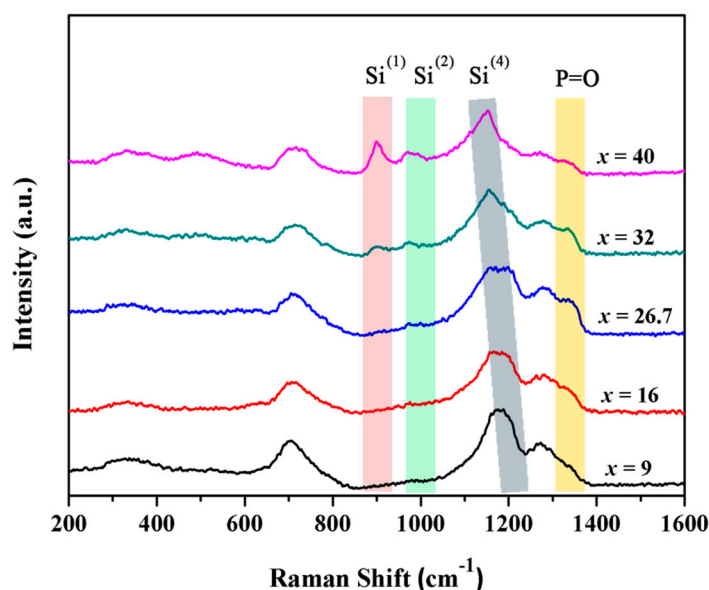


Figure 4. Micro-Raman spectra of $20\text{BaO}-(80-x)\text{P}_2\text{O}_5-x\text{SiO}_2-1\text{Yb}_2\text{O}_3$ ($x = 9, 16, 26.7, 32,$ and 40 mol %, respectively) glasses.

4. Conclusions

The influence mechanism of SiO_2 on the structural and spectroscopic properties of phosphate glasses prepared by the conventional melt-quenching method was systematically investigated using the micro-Raman technique and previous ^{29}Si MAS NMR analysis. A significant change occurs in the variation trends of fluorescence lifetimes and the scalar crystal-field N_j , and Yb^{3+} asymmetry degree when the SiO_2 content is greater than 26.7 mol %. It is worth noting that the glass with 26.7 mol % SiO_2 possess the longest fluorescence lifetime (1.51 ms), the highest gain coefficient ($1.10 \text{ ms}\cdot\text{pm}^2$), the maximum Stark splitting manifold of $^2\text{F}_{7/2}$ level (781 cm^{-1}), and the greatest N_j and Yb^{3+} asymmetry degree. Micro-Raman spectra indicate that the formation of P=O linkages in the glass is responsible for this abnormal variation. With the increase in the SiO_2 concentration, the intensity of the P=O linkages increases, and then slightly decreases when the SiO_2 content is greater than 26.7 mol %. This variation trend is consistent with the N_j and Yb^{3+} asymmetry degree. Additionally, based on the previous ^{29}Si MAS NMR experimental results, $[\text{SiO}_6]$ units existing in these phosphosilicate glasses may significantly affect the formation of P=O, and thus influence the spectroscopic properties of the glasses. It can be realized that these phosphosilicate glasses could be materials possessing the potential to be developed as a Yb^{3+} -doped gain medium for high-power solid-state lasers and broadband optical amplifiers.

Acknowledgments: This work was financially supported by the National Natural Science Foundation of China (No. 51572082, No. 21476083), the Major Program of Science and Technology Commission of Shanghai Municipality (No. ZD14521100604), the Fundamental Research Funds for the Central Universities (No. WD1313009), and the Open Fund of the Key Laboratory for Ultrafine Materials of the Ministry of Education at East China University of Science and Technology. Furthermore, we would like to thank Liyan Zhang (Key Laboratory of Materials for High Power Laser, Shanghai Institute of Optics and Fine Mechanics, Chinese Academy of Sciences) for helpful discussions.

Author Contributions: The manuscript was written through contributions of all authors. Huidan Zeng and Ling Wang conceived and designed the experiments; Ling Wang, Feng Ye, and Bin Yang performed the experiments; Huidan Zeng, Ling Wang, Jianding Chen, Guorong Chen, Andrew T. Smith and Luyi Sun analyzed the experimental results. Huidan Zeng and Ling Wang wrote the manuscript. All the authors have given approval to the final version of the manuscript.

Conflicts of Interest: The authors declare no conflict of interest.

References

1. Zou, X.; Toratani, H. Evaluation of spectroscopic properties of Yb³⁺-doped glasses. *Phys. Rev. B* **1995**, *52*, 15889–15897. [[CrossRef](#)]
2. Eger, D.; Atar, G.; Bruner, A.; Sfez, B.; Juwiler, I.; Kokki, T.; Kykkänen, P. Spectral characterization of Yb-doped silica layers for high power laser applications. *Opt. Mater.* **2011**, *33*, 438–443. [[CrossRef](#)]
3. Zhang, L.; Pan, W.; Feng, J. Dependence of spectroscopic and thermal properties on concentration and temperature for Yb:Y₂O₃ transparent ceramics. *J. Eur. Ceram. Soc.* **2015**, *35*, 2547–2554. [[CrossRef](#)]
4. Hönninger, C.; Paschotta, R.; Graf, M.; Morier-Genoud, F.; Zhang, G.; Moser, M.; Biswal, S.; Nees, J.; Braun, A.; Mourou, G.A.; et al. Ultrafast ytterbium-doped bulk lasers and laser amplifiers. *Appl. Phys. B* **1999**, *69*, 3–17. [[CrossRef](#)]
5. DeLoach, L.D.; Payne, S.A.; Chase, L.L.; Smith, L.K.; Kway, W.L.; Krupke, W.F. Evaluation of absorption and emission properties of Yb³⁺-doped crystals for laser applications. *IEEE J. Quantum Electron.* **1993**, *29*, 1179–1191. [[CrossRef](#)]
6. Snitzer, E. Optical maser action of Nd³⁺ in a barium crown glass. *Phys. Rev. Lett.* **1961**, *7*, 444–446. [[CrossRef](#)]
7. Jiang, C.; Liu, H.; Zeng, Q.J.; Tang, X.D.; Gan, F.X. Yb: Phosphate laser glass with high emission cross-section. *J. Phys. Chem. Solids* **2000**, *61*, 1217–1223. [[CrossRef](#)]
8. Dai, S.X.; Sugiyama, A.; Hu, L.L.; Liu, Z.P.; Huang, G.S.; Jiang, Z.H. The spectrum and laser properties of ytterbium doped phosphate glass at low temperature. *J. Non-Cryst. Solids* **2002**, *311*, 138–144. [[CrossRef](#)]
9. Krishnaiah, K.V.; Jayasankar, C.K.; Chaurasia, S.; Murali, C.G.; Dhareshwar, L.J. Preparation and characterization of Yb³⁺-doped metaphosphate glasses for high energy and high power laser applications. *Sci. Adv. Mater.* **2013**, *5*, 1–9. [[CrossRef](#)]
10. Hu, J.Y.; Yang, H.W.; Chen, Y.J.; Lin, J.S.; Lai, C.H.; Lee, Y.M.; Zhang, T. Properties and structure of Yb³⁺ doped zinc aluminum silicate phosphate glasses. *J. Non-Cryst. Solids* **2011**, *357*, 2246–2250. [[CrossRef](#)]
11. Chen, Y.K.; Wen, L.; Hu, L.L.; Chen, W.; Guyot, Y.; Boulon, G. Raman and optical absorption spectroscopic investigation of Yb-Er codoped phosphate glasses containing SiO₂. *Chin. Opt. Lett.* **2009**, *7*, 56–59. [[CrossRef](#)]
12. Wang, P.; Wang, C.; Hu, L.L.; Zhang, L.Y. Effect of SiO₂ on the Stark splitting enlargement of Yb³⁺ in phosphate glass. *Acta Phys. Sin.* **2016**, *5*, 311–317.
13. Li, X.; Zeng, H.D.; Ye, F.; Chen, J.D.; Chen, G.R.; Chen, D.P. Influence of SiO₂ on the Luminous Properties of Nd³⁺-Doped Barium Silicophosphate. *Nanosci. Nanotechnol. Lett.* **2016**, *8*, 207–210. [[CrossRef](#)]
14. Xu, W.B.; Ren, J.J.; Shao, C.Y.; Wang, X.; Wang, M.; Zhang, L.Y.; Chen, D.P.; Wang, S.K.; Yu, C.L.; Hu, L.L. Effect of P⁵⁺ on spectroscopy and structure of Yb³⁺/Al³⁺/P⁵⁺ co-doped silica glass. *J. Lumin.* **2015**, *167*, 8–15. [[CrossRef](#)]
15. McCumber, D.E. Einstein Relations connecting broadband emission and absorption spectra. *Phys. Rev.* **1964**, *136*, A954–A957. [[CrossRef](#)]
16. Yin, H.B.; Deng, P.Z.; Zhang, J.Z.; Gan, F.X. Determination of emission cross section of Yb³⁺ in glasses by the reciprocity method. *Mater. Lett.* **1997**, *30*, 29–33. [[CrossRef](#)]
17. Dai, S.X.; Hu, L.L.; Sugiyama, A.; Izawa, Y.; Liu, Z.P.; Jiang, Z.H. Study of a new ytterbium doped phosphate laser glass. *Chin. Sci. Bull.* **2002**, *47*, 255–259. [[CrossRef](#)]
18. Auzel, F. On the maximum splitting of the (²F_{7/2}) ground state in Yb³⁺-doped solid state laser materials. *J. Lumin.* **2001**, *93*, 129–135. [[CrossRef](#)]

19. Xu, W.B.; Yu, C.L.; Wang, S.K.; Lou, F.G.; Feng, S.Y.; Wang, M.; Zhou, Q.L.; Chen, D.P.; Hu, L.L.; Guzik, M.; et al. Effects of F^- on the optical and spectroscopic properties of Yb^{3+}/Al^{3+} co-doped silica glass. *Opt. Mater.* **2015**, *42*, 245–250. [[CrossRef](#)]
20. Yang, B.H.; Liu, X.Q.; Wang, X.; Zhang, J.J.; Hu, L.L.; Zhang, L.Y. Compositional dependence of room-temperature Stark splitting of Yb^{3+} in several popular glass systems. *Opt. Lett.* **2014**, *39*, 1772–1774. [[CrossRef](#)] [[PubMed](#)]
21. Aguiar, H.; Serra, J.; González, P.; León, B. Structural study of sol gel silicate glasses by IR and Raman spectroscopies. *J. Non-Cryst. Solids* **2009**, *355*, 475–480. [[CrossRef](#)]
22. Dupree, R.; Holland, D.; Mortuza, M.G. Six-coordinated silicon in glasses. *Nature* **1987**, *328*, 416–417. [[CrossRef](#)]
23. Yamashita, H.; Yoshino, H.; Nagata, K.; Yamaguchi, I.; Ookawa, M.; Maekawa, T. NMR and Raman Studies of $Na_2O-P_2O_5-SiO_2$ Glasses. *J. Ceram. Soc. Jpn.* **1998**, *106*, 539–544. [[CrossRef](#)]
24. Zeng, H.D.; Jiang, Q.; Liu, Z.; Li, X.; Ren, J.; Chen, G.R.; Liu, F.D.; Peng, S. Unique sodium phosphosilicate glasses designed through extended topological constraint theory. *J. Phys. Chem. B* **2014**, *118*, 5177–5183. [[CrossRef](#)] [[PubMed](#)]
25. Hudgens, J.J.; Brow, R.K.; Tallant, D.R.; Martin, S.W. Raman spectroscopy study of the structure of lithium and sodium ultraphosphate glasses. *J. Non-Cryst. Solids* **1998**, *223*, 21–31. [[CrossRef](#)]
26. Plotnichenko, V.G.; Sokolov, V.O.; Koltashev, V.V.; Dianov, E.M. On the structure of phosphosilicate glasses. *J. Non-Cryst. Solids* **2002**, *306*, 209–226. [[CrossRef](#)]
27. Ji, X.M.; Zeng, H.D.; Li, X.; Ye, F.; Chen, J.D.; Chen, G.R. High glass transition temperature barium silicophosphate glasses designed with topological constraint theory. *J. Am. Ceram. Soc.* **2016**, *99*, 1255–1258. [[CrossRef](#)]



© 2017 by the authors. Licensee MDPI, Basel, Switzerland. This article is an open access article distributed under the terms and conditions of the Creative Commons Attribution (CC BY) license (<http://creativecommons.org/licenses/by/4.0/>).